ISSN (Print) 1226-1750
ISSN (Online) 2233-6656
Journal of Magnetics 18(3), 331-338 (2013) http://dx.doi.org/10.4283/JMAG.2013.18.3.331

Recent Developments in Magnetic Measurements: from Technical Method to Physical Knowledge

V. Basso, F. Fiorillo*, C. Beatrice, A. Caprile, M. Kuepferling, A. Magni, and C. P. Sasso

Istituto Nazionale di Ricerca Metrologica - INRIM, 10135 Torino, Italy

(Received 1 June 2012, Received in final form 16 November 2012, Accepted 16 November 2012)

We present a few significant advances in methods and concepts of magnetic measurements, aimed both at providing novel routes in the characterization of hard and soft magnetic materials and at improving our basic knowledge of the magnetization process. We discuss, in particular, investigation methods and experimental arrangements that have been developed in recent times for: 1) Hysteresis loop determination in extra-hard magnets by means of Pulsed Field Magnetometry; 2) Broadband observation of domain wall dynamics by high-speed stroboscopical Kerr techniques; 3) Entropy measurements in magnetocaloric materials by calorimetry in magnetic field. While pertaining to somewhat independent fields of investigation, all these measuring techniques have in common a solid approach to the underlying physical phenomenology and have a potential for further developments.

Keywords : magnetic measurements, pulsed field magnetometry, magneto-optics, magnetocaloric effect

1. Introduction

Study, processing, applications, and commerce of magnetic materials all call for precise measurements. These must rely on solid physical foundations and, when close to applications, they must be traceable to the appropriate standards. The appearance of novel physical phenomena and new or improved materials, and the development of increasingly fast digital methods in measurement control and data acquisition/handling have brought about new challenges and opportunities in magnetic measurements. For example, the modern rare-earth based extra-hard permanent magnets cannot be exhaustively tested using the standard electromagnet based approach, which is limited by the saturation of iron [1, 2]. The Pulsed Field Magnetometry (PFM), where the specimens can be subjected to transient fields high enough to bring the material to saturation, has therefore been developed as a viable alternative.

The compelling need for high-frequency magnets, driven by their increasing applications in devices converting and manipulating electromagnetic signals up to the GHz range, calls for physical insight into the magnetization process under such extreme conditions. Recently introduced ultra-fast magneto-optical techniques [3] permit one to directly observe the time dependent magnetization process down to picosecond resolution [4]. Early damping of domain wall relaxation with increasing frequency is observed in thin metallic plates if rotations can simultaneously occur [5].

For magnetic compounds with Curie temperature close to room temperature, appreciable entropy variation can be obtained under a changing magnetic field. It is the magnetocaloric effect. Magnetic refrigeration is therefore envisaged and, with this prospective goal in mind, a number of special measuring techniques have been developed to study the magnetocaloric phenomena [6-8].

We shall provide in the following a discussion on recent results regarding PFM, magnetocaloric, and fast magneto-optical investigations. We shall look, in particular, at the physical insight gained by application of these techniques, besides highlighting their technical features and perspectives. They find common ground in their objective of providing novel information, assessed in a solid physical framework, on the phenomenology of materials having somewhat extreme or special properties: very high coercivities, high magnetocaloric effect, very low losses at high

*Corresponding author: Tel: +390113919836
Fax: +390113919834, e-mail: f.fiorillo@inrim.it

This paper was presented at the ICM2012, Busan, Korea, July 8-13, 2012.

frequencies, etc.. While a description of the present state of the art in magnetic measurements would be outside the limited scope of this review, the selected examples will possibly convey trends and ideas lying behind recent advances in experimental methods, an indispensable step in the road to improved materials and applications.

2. Pulsed Field Magnetometry in Permanent Magnets

Rare-earth based materials, the most performing permanent magnets nowadays available, are endowed with very high coercivities, typically exceeding 1×10^6 A/m, and can be characterized only to a limited extent using the standard methods, which call for closed circuit configuration with an electromagnet [1, 2]. This limitation occurs because the iron yoke can saturate before reversing the magnetization of the permanent magnet under test, thereby engendering poor flux closure and strongly inhomogeneous field in the gap. Sufficiently high homogeneous fields can actually be achieved by open sample measurements using a superconducting field source, but implementation of a magnetometer (either of vibrating sample or extraction types [9]) using this source is of little appeal from the industrial viewpoint, given its intrinsic complexity and the high running costs of liquid helium. It has therefore been suggested that a conventional room-temperature solenoid, supplied in a transient mode by the discharge of a condenser bank, can provide high-strength homogeneous field, by which all present-day industrial rare-earth based magnets can be brought to saturation [10, 11]. A Pulsed Field Magnetometer (PFM) can therefore be built around this principle. It consists of a solenoid source, by which a magnetic field of peak amplitude around several MA/m can be applied to the test specimen, a number of suitable pick-up coils, and a high-resolution system for acquisition and treatment of the detected signals. The field pulse can either be a simple transient, by which the magnet is brought to saturation and, subsequently, to the remanent state, or of oscillating damped type, leading to a sequence of hysteresis loops of progressively decreasing amplitude [12]. Fig. 1 illustrates two possible configurations of a PFM setup, as developed for testing permanent magnets according to a magnetometric (Fig. 1a) and a fluxmetric (Fig. 1b) approach, respectively [13]. For the specific apparatus of Fig. 1, a 170 mm long exciting solenoid of inductance L = 0.85 mH and bore diameter 50 mm has been employed. The peak field strength, obtained for an oscillatory pulse of period T = 11 ms (see Fig. 1) at the time $t = T/4$, can be as high as 6×10^6 A/m, sufficient to achieve the practical saturation of

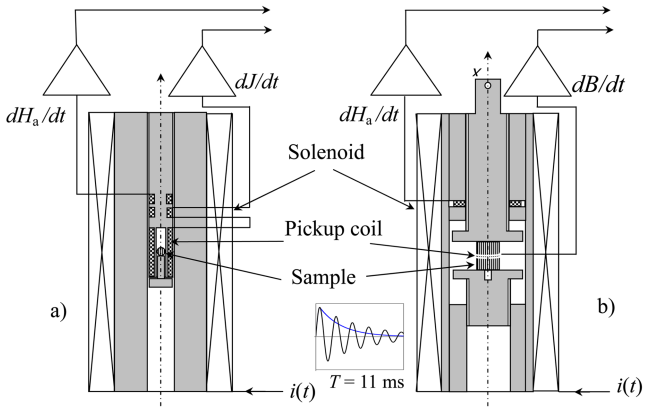

Fig. 1. (Color online) PFM setups for the measurement of the hysteresis loop in permanent magnets according to the magnetometric (a) and fluxmetric (b) methods [13].

the rare-earth compounds, according to the rules prescribed in the ASTM and IEC Standards [1, 2]. With the configuration of Fig. 1a, the magnetic moment m of a small spherical sample (diameter D = 2-4 mm) is measured versus time upon the application of the oscillating field pulse $H_a(t)$. To this end, the flux $\Phi = k_x m$ linked to a high-aspect ratio calibrated axial pickup coil of known constant k_x surrounding the specimen is measured. Instrumental to the precise determination of m is a very fine compensation of the linked air flux $\Phi_a = A\mu_0 H_a$, where A is the turn-area of the pickup coil. To this end, coaxial coils, placed far enough from the sample, are connected in series opposition to the sensing coil. The measurement is performed with and without the sample and numerically subtracting the obtained figures. Setup calibration is obtained by measuring a sample of known magnetic moment, in this case a Ba-ferrite sphere, previously tested in a calibrated VSM setup. The applied field is obtained by measuring the air-flux linked to a further axial coil. The fluxmetric configuration shown in Fig. 1b is applied to cylindrical/parallelepipedic samples, with maximum diameter/lateral size limited by the bore size. In this case the induction derivative $dB(t)/dt$ at midplane is detected by a few-turn localized coil, directly wound on the sample (wire diameter around 0.1 mm), and $H_a(t)$ is obtained as in the previous case. The setup is completed by low-noise signal amplifiers, high-resolution synchronous A/D converters, and software, eventually leading to the (B, H_{eff}) and (J, H_{eff}) hysteresis loops, with magnetic polarization J and effective field H_{eff} given by

$$J(t) = (B(t) - \mu_0 H_a(t))/(1 - \langle N_d \rangle)$$
$$H_{eff}(t) = H_a(t) - (\langle N_d \rangle/\mu_0) J(t)\,, \qquad (1)$$

The quantity $<N_d>$ stands for the demagnetizing factor $<N_d> = 1/3$ and for the fluxmetric demagnetizing factor at sample midplane in the magnetometric and fluxmetric measurements, respectively.

A merit of the PFM approach to permanent magnet testing is that of bringing to light the time effects in the measurement. Such effects, generally neglected in standard measurements, where the involved cycling period can run from a few ten to a few thousand seconds, become apparent on passing to the few millisecond measuring time of the PFM method. They are related to the thermal fluctuation aftereffect (magnetic viscosity) and, in sufficiently large and conductive samples, to eddy currents. The fluctuation aftereffect defines the phenomenon of thermally assisted magnetization reversal, generally interpreted in terms of a random internal fluctuation field of thermal origin. With shorter measuring times the measured coercivity H_c does slightly increase. On comparing the $T > 100$ s with the $T \sim 10$ ms experiments in a range of hard magnets, we find that such an increase ΔH_{cv} is proportional to H_c, according to the law $\Delta H_{cv} = 7 \times 10^{-2} H_c$ [13]. This is what we find for insulating materials (e.g. hard ferrites) and small conducting samples (i.e. the Nd-Fe-B and Sm-Co cylinders with diameter $D < 10$ mm). With larger conducting samples the eddy currents engender a further coercivity increase ΔH_{ce}. An example is provided in Fig. 2, showing the PFM loops measured in differently sized samples of a same Nd-Fe-B magnet. The $D = 13$ mm loop is slightly swollen by eddy currents. It is noted a transition at remanence, due to a magnetically soft surface layer, the smaller the sample the larger the kink. It is remarkable, however, that using a classical calculation, the effect of eddy currents on the loop shape can be easily corrected in cylindrical samples, where an analytical formulation for the eddy current field $<H_{eddy}(t)>$ is obtained [13]. The parametric equations for the eddy-current free hysteresis loop are obtained as

$$J(t) = \frac{\lfloor B(t) - \mu_0 H_a(t) - \mu_0 <H_{eddy}(t)> \rfloor}{1 - <N_d>}$$

$$H_{eff}(t) = H_a(t) - \frac{<N_d>}{\mu_0} J(t) + <H_{eddy}(t)>. \qquad (2)$$

Fig. 3 shows an example of retrieval of the hysteresis loop, as it would be obtained with a long measuring time, from the fast PFM loop in the case of a very large diameter Nd-Fe-B cylinder (D = 28.5 mm).

In the case of very fast magnetization dynamics, direct information of the magnetization process can be achieved by time resolved high-speed magneto-optics, as discussed in the next Section.

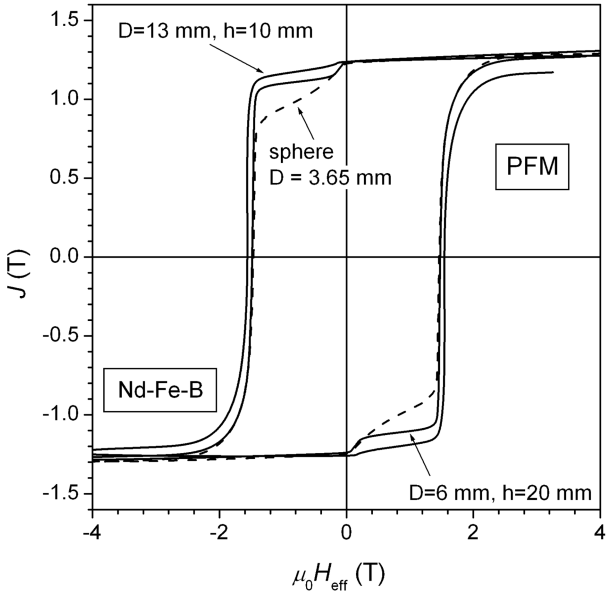

Fig. 2. Hysteresis loops measured in spherical (magnetometric) and cylindrical (fluxmetric) samples of a same Nd-Fe-B compound. A measurable increase of the measured coercive field, due to eddy currents, is observed in the 13 mm diameter sample.

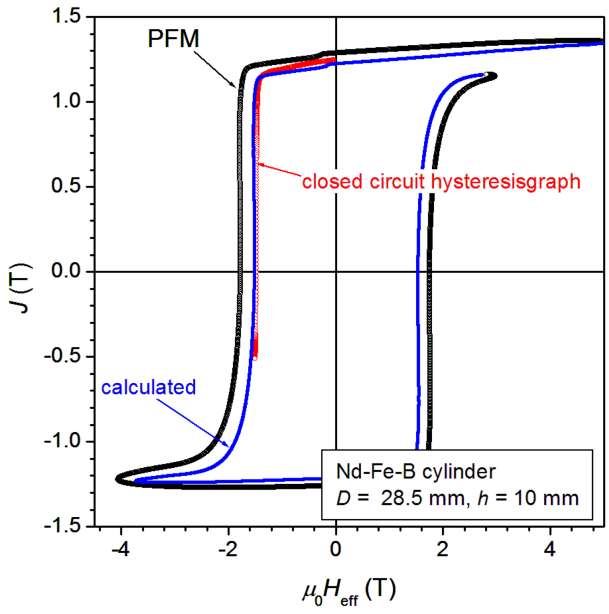

Fig. 3. (Color online) The hysteresis loop determined by PFM in a 28.5 mm diameter Nd-Fe-B cylindrical sample (conductivity $\sigma = 6.95 \times 10^5\ \Omega^{-1}\cdot m^{-1}$) is corrected for the combined effects of magnetic viscosity and eddy currents and the long measuring time ($T > 100$ s) loop is retrieved. This is compared in the second quadrant with the return curve obtained by the standard closed circuit method.

3. Fast Magneto-optics: A Direct Approach to the High-frequency Magnetization Process

The direct observation of the magnetic domains by the magneto-optical Kerr technique stems from the rotation of the plane of polarization of a light beam upon reflection from the surface of a magnetic sample. The amount of rotation depends on the relative directions of the local magnetization and the plane of incidence of the incoming light [14]. By this technique one can obtain something of a local hysteresisgraph, probing the magnetic hysteresis in regions as small as the microscope resolution $\lambda/2n$, where λ is the wavelength used, and n is the objective numerical aperture. But one can also proceed to acquire real time images of the magnetization evolution, an option made possible by the development of fast digital image processing. To note the possibility of making vector measurements [15] and depth-selective microscopy [16], which increase the amount of information. The latter, in particular, permits one to observe the domain structure at a given depth (within about 50 nm maximum depth). An obvious drawback of the Kerr analysis is the 50 nm maximum penetration depth of the visible light, which may not be a problem, however, in many thin film and thin plate samples, where surface and bulk domain structures coincide. Visible light also entails a maximum spatial resolution around 300 nm. This limit can be overcome, for example, with X-ray circular dichroism experiments [17].

The study of magnetic materials at high working frequencies is indispensable for a multitude of applications, propelled by the increasing need for the highest speed in detection, conversion, transmission, and general manipulation of electromagnetic signals. In doing so, one eventually approaches ferromagnetic resonance and, beyond that, a waning material response. The investigation of magnetization dynamics at high frequencies starts from the Landau-Lifschitz-Gilbert (LLG) equation, which describes the magnetization precession and the effect of damping on its motion. One of the first accomplishments of the stroboscopic methods has been the direct observation of the magnetization relaxation according to the LLG dynamics [18]. By investigating in the frequency range were stroboscopic methods can be applied we observe dynamical effects similar to those we are familiar with in the quasi-static regime, such as domain wall motion or nucleation of domains, but we also encounter new phenomena that require new theoretical approaches, such as fast switching by magnetization precession [19] [20], spin waves (magnetostatic, exchange, ...) [21], (whose spectrum can be continuous, or discrete in structured samples [22]), interaction of spin waves with domain walls and/or with spin polarized currents [23].

In a stroboscopic setup [24] the sample surface is observed during a very short time interval, whose position along the magnetization cycle is suitably imposed via a trigger signal, synchronous with the magnetizing field. In order to attain acceptable signal-to-noise ratio, the exposition is repeated during successive cycles, under the same trigger conditions, and averaging is performed. The time delay is then changed and the procedure repeated at another point along the period. It has been shown that using exposition times of the order of the laser pulse length ($\sim 10^{-13}$ s) one can investigate spin relaxation processes in great detail [25]. It is stressed that the requirement of repeatable magnetization process upon successive cycles, indispensable for applying the stroboscopic method, is typically satisfied at high frequencies. In a widely used stroboscopic method (Fig. 4), a pulsed light beam is split into pump and probe beams. The pump beam is used to trigger the system excitation, using a photodiode or an Auston switch. Once closed, the circuit sends a voltage pulse into a waveguide that generates a pulsed exciting field. At the same time, the probe beam is used to per-

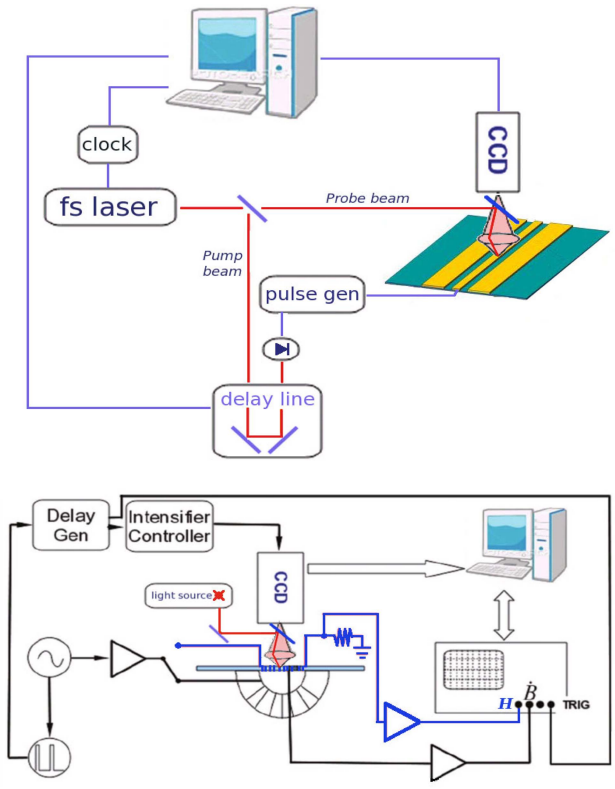

Fig. 4. (Color online) Stroboscopic wide-band setup (top) and camera-based (bottom) for time-resolved magneto-optical observations.

form the magneto-optical observation. The light sources commonly used are pulsed lasers, whose pulse width can reach values as low as 0.030 ps. The observation is performed on the sample surface by scanning it with a piezo-driven stage, acquiring at each spot the Kerr amplitude and reconstructing the magnetic image at a given field [26].

Stroboscopic methods based on the triggering capacities of the camera are possible, especially if the camera uses a gateable image intensifier (Fig. 4). This increases the light sensitivity and works as an extremely fast shutter, with aperture times as low as 50 ps. We are therefore in a position to investigate the magnetization dynamics beyond the MHz range, for example via coplanar waveguides. Most successfully investigated materials were in the past the YIG garnets, through polar Kerr effect. YIGs are still of interest today, because their low damping constant allows for spin wave propagation upon distances of the order of a few mm [27]. A wide variety of materials are nowadays investigated, both as continuous films and patterned samples.

Time-resolved experiments in real time with nanosecond time resolution have led to the observation of the Walker breakdown in nanostrips [28]. In another experimental breakthrough, stroboscopic observations have been combined with pulsed inductive microwave magnetometry (PIMM), where the precessional dynamics of the magnetization is reconstructed by means of an inductive measurement at the same time as the Kerr measurement is performed [29]. The magnetic response can then be analyzed in the frequency domain, finding the resonance frequency as a function of a given DC field.

It is interesting to apply fast magneto-optic methods to novel materials and physical phenomena, like in the case of quantum dots (QD). Here Kerr spectroscopy with picosecond optical pulses has been performed [30]. Femtosecond pump-probe has also been applied to QD ensembles, where the pump pulses induce global coherent spin precession [31].

At very low timescales, the interpretation of the data is still not completely obvious. In the case of ultrafast demagnetization via femtosecond laser excitation [32], we have an out of equilibrium process with abrupt change of the magnetic properties of the material. In such a case the Kerr signal might possibly have weak connection with the local magnetization, because of the non-equilibrium electron distribution created by the pump pulse [33].

Very thin amorphous laminations, usually obtained in ribbon form, are a class of materials of great industrial interest, but we still lack a complete understanding of their magnetization properties in the MHz-GHz range. We know that the loss mechanisms active in this class of materials can be strongly influenced by magnetic anisotropy induced by field annealing at mild temperatures (250 °C - 300 °C). By creating, in particular, an anisotropy axis perpendicular to the ribbon length (i.e. to the applied field), we can obtain, especially in Co-based alloys, a combination of high permeability and low losses far superior to the one exhibited by the conventional Mn-Zn and Ni-Zn ferrites in a range of frequencies spanning from DC to 1 GHz [5, 34]. The key to this remarkable behavior is assumed to lie, besides the low value of the macroscopic magnetic anisotropy, in the progressive relaxation of the domain wall displacements with increasing frequency, their role being taken up by rotational processes. Direct observations of the domain wall dynamics versus frequency performed by fast stroboscopic Kerr method, permit one to validate this assumption, as illustrated by the image sequence shown in Fig. 5.

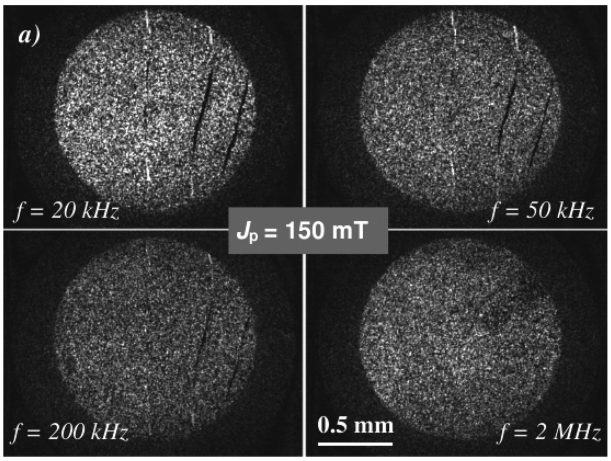

Fig. 5. As frequency takes the values f = 20 kHz, 50 kHz, 200 kHz, 2MHz, the area covered by domain wall displacements along a half-period (peak polarization value J_p = 150 mT) decreases. This is shown by the evolution of the differential magneto-optical images taken on a transverse anisotropy ($K_{u\perp}$ = 50 J/m^3) $Co_{71}Fe_4B_{15}Si_{10}$ amorphous ribbon with the camera-based setup shown in Fig. 4. The white and dark areas, corresponding to the regions covered by domain wall motion upon cycling (J_p = ± 150 mT) are observed to shrink with increasing f.

4. Calorimetry and the Magnetocaloric Effect

The possibility to develop refrigeration techniques in the solid state has directed numerous efforts towards existing or prospective materials with ferro-caloric effects, where the entropy can be changed by an external action, like the applied stress, the electric field, or the magnetic

field [35]. The magnetocaloric effect descends from the dependence of the system entropy $s(H_a,T)$ on the temperature T and the applied magnetic field H_a. In ferromagnets both the ferromagnetic exchange and the applied magnetic field contribute to create ordered spin configurations with low entropy. The magnetic field induced entropy change $\Delta s_{iso}(H_a)$ is thus found to be maximum at the magnetic phase transition temperature [36]. $Gd_4Si_2Ge_2$, $La(FeSi)_{13}$, and FeMn(PSi) with first order magnetic phase transitions, have been extensively studied for applications around room temperature [37-39].

To determine the magnetocaloric effect, several methods are employed. i) Magnetic measurements $M(H_a, T)$, where the isothermal entropy change Δs_{iso} is computed integrating the Maxwell relation $ds/dH_a = \mu_0 dM/dT$ [40]. This method applies well to systems with second order phase transitions, but it is not appropriate to transitions with temperature hysteresis [41]. ii) Adiabatic methods, where the temperature change ΔT_{ad} due to magnetic field is directly accessed [42]. iii) Calorimetry in magnetic field. In this case the specific entropy variation is computed from the measured heat flux q_s, by the expression

$$s - s_0 = \int_0^t \frac{q_s}{T_s} dt\,, \qquad (3)$$

where T_s is the sample temperature. This technique has the advantage that both Δs_{iso} and ΔT_{ad} are obtained from the $s(H_a, T)$ plot. From the experimental viewpoint, the heat flux calorimetry is appropriate in the presence of phase transitions of the first kind with latent heat. For use under magnetic fields generated by electromagnets, permanent magnets, and superconducting solenoids, many adaptations of the heat flow calorimetry principle have been proposed, including the use of miniaturized Peltier cells as heat flux sensors for samples of a few milligrams [43-46] and microcalorimetry chips for very small mass samples of a few micrograms [47, 48]. Peltier cells, with thermoelectric material generally made of $(Bi\text{-}Sb)_2(Te\text{-}Se)_3$ type semiconductors, are characterized by a proportionality factor between the measured voltage, v_P, and the heat flux, q_s, in the range 1-2.0 V/W and the typical heat flux sensitivity is around 1 μW. To determine the $s(H_a,T)$ diagram, the heat flux q_s to the sample can be measured either by temperature changes (temperature scan experiments) or magnetic field changes (isothermal experiments) [49]. The sample temperature T_s is evaluated measuring the temperature T of the thermal bath as $T_s = T - Rq_s$, where the thermal contact resistance R is a known quantity. The entropy $s(H_a,T)$ is computed from a temperature scan experiment under different magnetic fields using Eq. (3) and the relative vertical position of the curves is determined by isothermal experiments $\Delta s(H_a)_{T=const}$, where the magnetic field is changed at the constant temperature. Fig. 6 shows an example of measurements on hydrogenated $La(FeMnSi)_{13}$ prepared by Vacuumschmelze GmbH. These measurements were compared with other methods in [50]. Isothermal measurements of the entropy

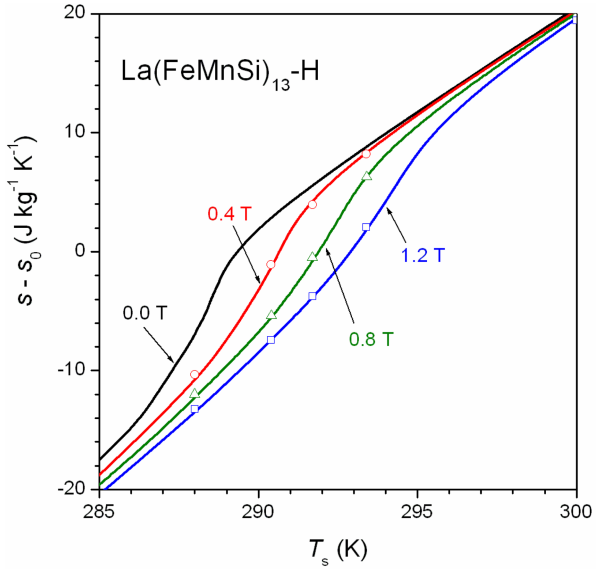

Fig. 6. (Color online) Entropy versus temperature under magnetic field measured by Peltier calorimetry on $La(FeMnSi)_{13}$-H prepared by Vacuumschmelze GmbH. Lines are given by temperature scan experiments, points are field scan experiments.

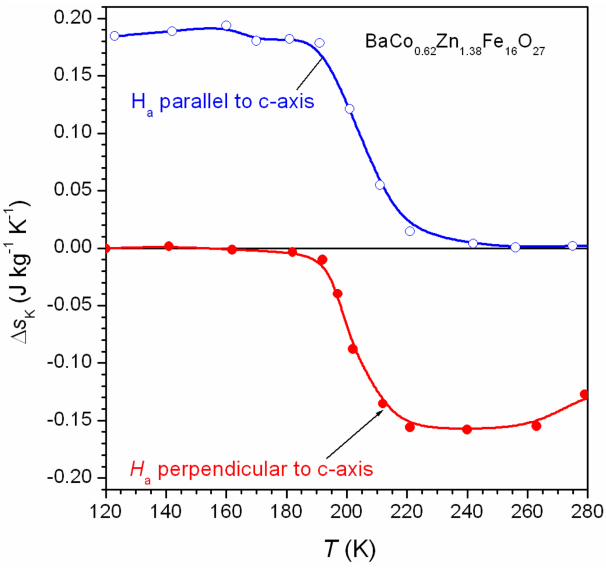

Fig. 7. (Color online) Magnetic field induced entropy change measured by Peltier calorimetry on a $BaCo_{0.62}Zn_{1.38}Fe_{16}O_{27}$ single crystal. The picture shows the spin reorientation contribution to the entropy change Δs_K obtained after subtraction of the ordinary effect from the measurement (after [51]).

change are also a sensitive method to characterize spin reorientation transitions [49, 51]. The entropy change associated with spin reorientation in transition metal oxides is generally very small (i.e. less than 1 $Jkg^{-1}K^{-1}$) and is hardly measurable by temperature scanning experiments, because it is superimposed to a large baseline due to uncompensated heat flux. On the contrary, the entropy difference between parallel and perpendicular magnetization can be obtained by measuring the entropy change induced by a magnetic field perpendicular to a local easy direction. In Fig. 7 we show experiments on a W-type ferrite single crystal of composition $BaCo_{0.62}Zn_{1.38}Fe_{16}O_{27}$ prepared by CNRS-Satie [51]. The magnetic field induced entropy change is due to the superposition of the ordinary magnetocaloric effect, proportional to dM_s/dT, and spin rotation contribution Δs_K proportional to dK_1/dT. After subtracting the first term [49, 51], we obtain the change $\Delta s_K = 0.18\ Jkg^{-1}K^{-1}$ between the low entropy easy plane state and the high entropy easy axis state.

5. Conclusions

We have reported about recent studies in experimental magnetism, focusing on physical insight and applicative perspectives. We have thus shown how by applying the Pulsed Field Magnetometry we can overcome the limitations posed by the standard test methods in the full characterization of the modern extra-hard rare-earth based permanent magnets. It is remarked that in this way the time effects, often neglected in the conventional measurements, can be brought to light and an encompassing view of the permanent magnet characterization can be obtained. We have then emphasized the increasingly powerful grasp of the dynamic features of the domain structure that can be achieved, up to microwave frequencies, by the development of fast magneto-optical techniques. Finally, we have touched upon the remarkable property of certain magnetic compounds of displaying a large entropy variation around room temperature and the array of measuring techniques for measuring its magnetic field dependence (magnetocaloric effect). By these techniques, one is not only able to bring forth new information on first-order and second-order magnetic phase transitions but can realize a platform for practical magnetic refrigeration.

References

[1] IEC Standard Publication 60404-5, Permanent Magnet (magnetically hard) Materials-Methods of Measurement of Magnetic Properties, Geneva: IEC Central Office, 1993.
[2] ASTM Publication A977/A977M-02, Standard test methods for magnetic properties of high-coercivity permanent magnet materials using hysteresigraphs, West Conshohocken, PA: ASTM International, 2002.
[3] D. Chumakov, J. McCord, R. Schäfer, L. Schultz, H. Vinzelberg, R. Kaltofen, and I. Mönch, Phys. Rev. B **71**, 014410 (2005).
[4] A. Neudert, J. McCord, D. Chumakov, R. Schäfer, and L. Schultz, Phys. Rev. B **71**, 134405 (2005).
[5] A. Magni, C. Beatrice, O. Bottauscio, A. Caprile, E. Ferrara, and F. Fiorillo, IEEE Trans. Magn. **48** (2012), in press.
[6] V. K. Pecharsky and K. A. Gschneidner, Jr., J. Appl. Phys. **86**, 565 (1999).
[7] K. P. Skokov, V. V. Khovaylo, K. H. Muller, J. D. Moore, J. Liu, and O. Gutfleisch, J. Appl. Phys. **111**, 07A910 (2012).
[8] V. Basso, M. Kuepferling, C. P. Sasso, and L. Giudici, Rev. Sci. Instrum. **79**, 063907 (2008).
[9] D. Dufeu and P. Lethuillier, Rev. Sci. Instr. **70**, 3035 (1999).
[10] R. Cornelius, J. Dudding, R. Grössinger, B. Enzberg-Mahlke, W. Fernengel, M. P. Knell, M. Küpferling, M. Taraba, J. C. Toussaint, A. Wimmer, and D. Edwards, IEEE Trans. Magn. **38**, 2462 (2002).
[11] P. Bretchko and R. Ludwig, IEEE Trans. Magn. **36**, 2042 (2000).
[12] F. Fiorillo, Measurement and Characterization of Magnetic Materials, Elsevier-Academic Press, Amsterdam (2004) p. 123.
[13] F. Fiorillo, C. Beatrice, O. Bottauscio, and E. Patroi, IEEE Trans. Magn. **43**, 3159 (2007).
[14] A. Hubert and R. Schaefer, Magnetic Domains Springer-Verlag, 2000.
[15] W. Rave, R. Schaefer, and A. Hubert, J. Magn. Magn. Mater. **65**, 7 (1987).
[16] R. Schaefer, J. Magn. Magn. Mater. **148**, 226 (1995).
[17] U. Hillebrecht, Science **284**, 2099 (1999).
[18] W. K. Hiebert, A. Stankiewicz, and M. R. Freeman Phys. Rev. Lett. **79**, 1134 (1997).
[19] M. Bauer, J. Fassbender, B. Hillebrands, and R. L. Stamps, Phys. Rev. B **61**, 3410 (2000).
[20] G. Bertotti, I. D. Mayergoyz, C. Serpico, and M. d'Aquino, IEEE Trans. Magn. **39**, 2501 (2003).
[21] D. D. Stancil, Spin Waves: Theory and Applications, Springer-Verlag, New York (2009).
[22] Spin Dynamics in Confined Magnetic Structures, B. Hillebrands and K. Ounadjela, eds., Springer, New York (2002).
[23] K. Sekiguchi, K. Yamada, S. Seo, K. Lee, D. Chiba, K. Kobayashi, and T. Ono, Phys. Rev. Lett. **108**, 017203 (2012).
[24] R. Schaefer, in Handbook of Magnetism and Advanced Magnetic Materials, Vol. 3, H. Kronmuller and S. Parkin, eds. Wiley, Chichester (UK) (2007).
[25] P. S. Keatley, V. V. Kruglyak, P. Gangmei, and R. J. Phil,

Trans. R. Soc. A **369**, 3115 (2011).
[26] M. R. Freeman and W. K. Hiebert, in Spin Dynamics in Confined Magnetic Structures, B. Hillebrands and K. Ounadjela, eds., Springer, New York (2002).
[27] A. Serga, A. Chumak, and B. Hillebrands, J. Phys. D **43**, 264002 (2010).
[28] C. Nistor, G. S. D. Beach, and J. L. Erskine, Rev. Sci. Instrum. **77**, 103901 (2006).
[29] U. Queitsch, J. McCord, A. Neudert, R. Schaefer, L. Schultz, K. Rott, and H. Brückl, J. Appl. Phys. **100**, 093911 (2006).
[30] J. Berezovsky, M. H. Mikkelsen, N. G. Stoltz, L. A. Coldren, and D. D. Awschalom, Science **320**, 349 (2008).
[31] A. Greilich, A. Shabaev, D. R. Yakovlev, Al. L. Efros, I. A. Yugova, D. Reuter, A. D. Wieck, and M. Bayer, Science **317**, 1896 (2007).
[32] B. Koopmans, G. Malinowski, F. Dalla Longa, D. Steiauf, M. Fähnle, T. Roth, M. Cinchetti, and M. Aeschlimann, Nature Materials **9**, 259 (2010).
[33] K. Carva, M. Battiato, and P. M. Oppeneer, Nature Physics **7**, 665 (2011).
[34] A. Magni, F. Fiorillo, A. Caprile, E. Ferrara, and L. Martino, J. Appl. Phys. **109**, 07A322 (2011).
[35] S. Fahler, U. K. Roessler, O. Kastner, J. Eckert, G. Eggeler, H. Emmerich, P. Entel, S. Mueller, E. Quandt, and K. Albe, Adv. Eng. Mater. **14**, 10 (2012).
[36] A. M. Tishin and Y. I. Spichkin, The magnetocaloric effect and its applications, IOP Publishing, Bristol (2003).
[37] K. A. Gschneidner Jr., V. K. Pecharsky, and A. O. Tsokol, Rep. Prog. Phys. **68**, 1479 (2005).
[38] E. Bruck, O. Tegus, D. T. Cam Thanh, Nguyen T. Trung, and K. H. J. Buschow, Int. J. Refrigeration **31**, 763 (2008).
[39] B. G. Shen, J. R. Sun, F. X. Hu, H. W. Zhang, and Z. H. Cheng, Adv. Mater. **21**, 4545 (2009).
[40] V. K. Pecharsky and K. A. Gschneidner, Jr, J. Appl. Phys. **86**, 565 (1999).
[41] V. Basso, M. Kuepferling, C. P. Sasso, and L. Giudici, Rev. Sci. Instrum. **79**, 063907 (2008).
[42] K. P. Skokov, V. V. Khovaylo, K.-H. Muller, J. D. Moore, J. Liu, and O. Gutfleisch, J. Appl. Phys. **111**, 07A910 (2012).
[43] T. Plackowski, Y. Wang, and A. Junod, Rev. Sci. Instrum. **73**, 2755 (2002).
[44] J. Marcos, F. Casanova, X. Batlle, A. Labarta, A. Planes, and L. Manosa, Rev. Sci. Instrum. **74**, 4768 (2003).
[45] S. Jeppesen, S. Linderoth, N. Pryds, L. Theil Kuhn, and J. Buch Jensen, Rev. Sci. Instrum. **79**, 083901 (2008).
[46] V. Basso, C. P. Sasso, and M. Kuepferling, Rev. Sci. Instrum. **81**, 113904 (2010).
[47] A. A. Minakov, S. B. Roy, Y. V. Bugoslavsky, and L. F. Cohen, Rev. Sci. Instrum. **76**, 043906 (2005).
[48] A. F. Lopéandia, E. André, J.-L. Garden, D. Givord, and O. Bourgeois, Rev. Sci. Instrum. **81**, 053901 (2010).
[49] V. Basso, C. P. Sasso, M. Kuepferling, K. P. Skokov, and O. Gutfleisch, J. Appl. Phys. **109**, 083910 (2011).
[50] K. Morrison, K. G. Sandeman, L. F. Cohen, C. P. Sasso, V. Basso, A. Barcza, M. Katter, J. D. Moore, K. P. Skokov, and O. Gutfleisch, Int. J. Refrigeration (2012), in press.
[51] M. LoBue, V. Loyau, F. Mazaleyrat, A. Pasko, V. Basso, M. Kuepferling, and C. P. Sasso, J. Appl. Phys. **111**, 07A905 (2012).